An Experimental Investigation of the Consolidation Behaviour of Un-cured Prepregs under Processing Conditions

O. J. Nixon-Pearson[a]*, J. P.-H. Belnoue[a], D. S. Ivanov[a], K. D. Potter[a], S. R. Hallett[a]

[a]University of Bristol, Advanced Composites Centre for Innovation and Science, Queens Building, University Walk, Bristol, BS8 1TR.
**corresponding author: on5405@bristol.ac.uk*

Abstract

This paper presents a methodology and research study that characterises toughened materials, as is needed for optimisation of composite manufacturing processes. The specific challenge is to cover all of the stages of advanced composite manufacturing: fibre deposition by automatic fibre placement machines, hot or room temperature debulking, and consolidation in an autoclave. In these processes the material experiences a wide range of processing parameters: pressure, load rate, temperatures, and boundary constraints. In these conditions toughened prepregs, exhibit complex rheological behaviour, with diverse flow and deformation mechanisms at various structural scales. Here a series of experimental results are presented in order to describe the temperature, viscosity, flow mechanisms, and scale-effects of simple un-cured prepreg stacks. The driver for this study is to obtain a further understanding of flow mechanisms throughout the consolidation phase of composites manufacture since fibre path defects are most likely to occur during compaction, prior to vitrification.

Keywords: *Prepreg; Microstructures; Optical Microscopy; Consolidation; Manufacturing.*

1. Introduction

At present, in the drive for efficiency, cost and quality, the composite manufacturing industry faces various challenges to understand and control material behaviour throughout the production processes fibre deposition, debulking, consolidation, and curing. Currently optimisation efforts are mainly focussed on decreasing the time of debulking, preventing fibre path and impregnation defects, controlling fibre position/orientation, eliminating resin rich zones, reducing the weight of the component, and avoiding costly consolidation tooling.
Understanding the fundamental mechanical behaviour of prepregs during processing is crucial for optimisation of processing parameters and defect mitigation. Pre-impregnated fibres with a multiphase toughened resin (prepreg) is a highly complex system where the compliance of the fibres and inertia of the viscous matrix makes

them susceptible to fibre-matrix motion. Upon curing, the fibre paths and impregnation features become "locked" into the composite architecture. Any fibre path and impregnation defects at this stage can then dictate the subsequent mechanical performance. Toughening with thermoplastic particles introduces an extra phase to the material and, as a consequence, increases the complexity of the prepreg systems even further. The presence of a dissolved thermoplastic phase substantially extends the range of resin viscosity in the temperature processing range (up to five-six orders of magnitude (1)), undissolved thermoplastic changes surface topology and the mechanical properties of ply interfaces and impacts on flow and deformation mechanisms. Thus, it is fundamentally important to understand how the composite precursor material deforms during the processing operations to control composite dimensions, fibre volume fraction, resin rich zones, and fibre path defects.

A compliant network of fibres and viscous matrix exhibits various flow and deformation mechanisms depending on applied conditions (2). Two major factors in consolidation are bleeding/percolation flow, which is typical for low-viscosity thermoset resins, and shear/squeezing flow, mostly observed in consolidation of thermoplastic prepregs. In bleeding flow the pressure gradient causes resin flow relative to the fibres. Thus, the resin escapes from the laminate without moving the fibres in-plane but is accompanied by fibre bed compaction. In squeezing flow the system deforms as an incompressible fluid and the fibre-matrix system moves transverse to the fibre and compaction directions. In pure bleeding flow the through-thickness compaction is limited: it is determined by the ratio of initial fibre volume fraction (typically 40-50% after debulking) to the maximum fibre volume fraction (typically 70-75%). In the laterally unconstrained squeezing regime higher overall compressibility is possible due to the transverse flow of material.

One of the characteristic mechanisms of fibre path defect formation is local non-uniform consolidation, which leads to the generation of an excess length. This can result in the ply alignment angle then either rotating around the original fibre axis (defect known as "fold") or around the fibre transverse direction (defect known as "wrinkle"). The actuation of a particular mechanism depends on various factors including; resin viscosity, instant fibre volume fraction, pressure distribution, load rates, and constraints of the material. The mechanisms of flow in toughened prepregs may be switched within one processing step or through the entire chain of steps where a wide range of parameters is observed. Three main steps in automated composite processing are:

- High speed deposition (up to 1m/sec (3)) of thin tapes at relatively low temperature and moderate pressure.
- Slow debulking of stacked laminates at elevated temperature (30-90^{o}C) and atmospheric pressure.

- High pressure consolidation of material in autoclave under high pressure and temperature followed by resin vitrification and subsequent curing.

Characteristic values of parameters in these processes are summarised in Table 1.

Table 1. Indicative parameters of prepreg processing

	Automatic fibre deposition	Hot/cold debulking	Consolidation in autoclave
Temperature, °C	30-40	20-90	20-180
Pressure, MPa	0.1-0.2	0.1	0.7
Pressure rate, MPa/sec	up to 7	Slow	Slow
Characteristic dimensions	Tapes 6-12 mm in width, prepreg- roller contact length 30 mm	Component size	Component size
Time scale	0.03 sec	Minutes/Hours	Hours

Due to the viscoelastic-to-fluid phase transition arising from the dissolved thermoplastic, toughened prepregs exhibit features typical of both low-viscosity thermosets and high viscosity thermoplastics. For the compaction of angle ply laminates, Hubert and Poursartip (4) have showed that there is always some interaction between squeezing and percolation flow mechanisms, with percolation dominating under bleed conditions and squeezing flow dominating under no-bleed conditions. There have been various approaches to the testing of prepregs and pre-impregnated preforms, aimed at identifying material properties. The use of one or another technique is largely determined by the assumed flow mechanisms and requirements of models that these tests are usually aimed at providing input data for. Gutowski and Dillon (5) presented a large collection of data on fibre bed responses across studies on different materials. They concluded that: the limit fibre volume fractions in lubricated fibre bundles and prepregs are distinctly different, and the rate effects in consolidation of fibres are important. Hubert and Poursartip (6) suggested an experimental program for prepregs aiming to derive the elastic fibre bed response. A ramp-dwell programme was utilised to separate the pressure in the fibre bed from the time-dependent reaction of the resin. Bickerton and Buntain (7) conducted a similar experiment for the RTM process and found a different fibre bed response between the compaction of dry preforms and infused samples due to a lubrication effect. Kelly (8) suggested that a multiplicative superposition of elastic and rate-dependent material reaction could better describe their experimental data and proposed a series of monotonic compaction experiments to calibrate their material model. Lukaszewicz and Potter (9), investigating the behaviour of toughened prepreg under conditions of AFP, assuming time independent response of the material at high strain rates. The properties of an elasto-plastic model were then found by extrapolating the results of relaxation tests to high strain rates.

Hubert and Poursartip (4), tested toughened and low viscosity prepregs on curved tools with bleed and non-bleed bagging conditions. They clearly demonstrated that both squeezing and percolation flow mechanisms can act concurrently. Thus it will be of significant merit for further investigation at the coupon level. Typically the current state-of-the-art discussed above places emphasis on fibre bed response in order to extract fibre bed permeability and elastic response, as required by current modelling approaches.

This paper presents a series of experiments aimed at characterising in detail the main mechanisms of toughened prepregs' deformation. A new experimental methodology has been designed to:

- explore the compaction behaviour of uncured prepregs under processing conditions consistent with all the stages of composite processing: Automatic Fibre Deposition (AFP), cold or hot debulking and consolidation. The focus of the study is on prepreg consolidation, the combination of flow mechanisms, size effects, and the limit states.
- investigate the feasibility of deriving macro-properties from small scale coupon tests involving minimum of material and experimental efforts and assess the size effects in uncured material. Various laminate configurations are investigated to address the scale-effect issues;
- generate data for simple extraction of geometric material parameters in a robust procedure, covering all the temperature, pressure and pressure rate ranges for a 3D hyper-viscoelastic model by Belnoue et al. (10).

Most importantly this study also deviates away from standard conventions in which edges are fully blocked in order to reproduce the boundary conditions seen by a point situated in the middle of a large composite panel (6). The present study concentrates on non-bleed conditions representative what is happening at the ply edges and more generally in areas where fibre path defects are formed. This justifies why the ply edges are left unconstrained. In a second paper, the experimental results and observations presented here are used to build and validate a model representative of these conditions (10).

1.1 Materials and samples

Two toughened aerospace grade prepreg systems developed by Hexcel® were investigated; IM7/8552, with a nominal cured ply thickness of 0.125 mm, nominal fibre volume fraction of 57.7%, and a nominal resin content of 35% weight, and IMA/M21, with nominal cured ply thickness of 0.184 mm, nominal fibre volume fraction of 59.2%, and nominal resin content of 34% weight. These two systems represent characteristic material

toughening strategies. In the IM7/8552 carbon fibre/epoxy system, dissolved thermoplastic is dispersed within plies, throughout the bulk phase of the resin. The IMA/M21 system is designed to preserve an extra layer of thermoplastic particles as a distinct interleaf between the plies during processing. The thermoplastic phase is introduced to address the common problem of composite brittleness as it enhances the fracture toughness and impact performance of the laminate. At the same time thermoplastics affect the processing characteristics of the prepreg. Toughening elevates the prepreg's viscosity, changes inter-ply friction, and morphology, for example as shown by Lukaszewicz and Potter (11) for IMA/M21. As a result, the flow and deformation mechanisms are significantly affected. The steep drop in the viscosity of the resins from ambient temperature to gel point is a common characteristic in thermosetting resins as shown by Hubert et al (12). The rheological properties of the resin and the prepreg systems used here are well understood and are not repeated in this paper, for further details see (12-15).

All the tests are performed within the range of temperatures and time scales where the degree of cure does not evolve (maximum temperature 90°C and test duration did not exceed 15 min). As has been shown by Hubert et al (12) in an isothermal test, considerable change in viscosity of 8552 resin does not occur at 110°C at much longer time scales (above 60 minutes).

The specimen design for compaction testing of both prepreg systems followed that first presented by Ivanov et. al. (2) in which a cross-ply specimen is loaded under compression at various temperatures, pressures and pressure rates. One of the major requirements of the test programme was to reproduce ply-interaction conditions of a representative prepreg element, e.g. tape, within the laminate. Simple square shaped specimens tend to lose material from underneath the pressurised area due to transverse spreading as the plies are squeezed. Therefore the plies were laid up in a cruciform geometry to allow material that spreads laterally to remain in contact with plies above and below it, see – figure 1.

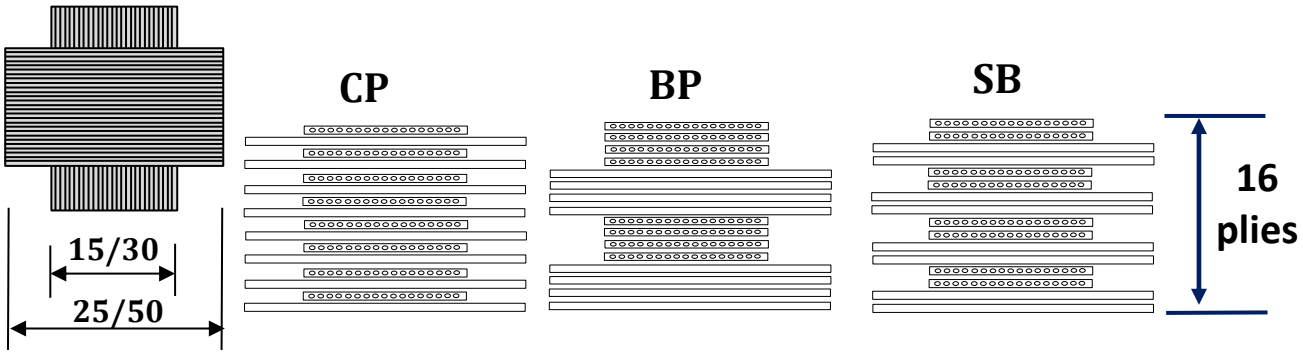

Figure 1. Plan view of baseline and scale-up specimens with cross section view of lay-up.

Another advantage of the free edge conditions was that they removed all the uncertainties related to constraining the material externally, which is difficult to impose ideally. The contact forces arising from constrained edges will be non-uniform around the specimen edges and likewise throughout the duration of processing, and will thus introduce a level of variability. It is also a requirement of the model development in (10). Thus the test does not reproduce the boundary conditions imposed on prepreg in the bulk of gap-free material but the material properties extracted from these tests can be used for modelling both constrained and free edge systems.
To explore size effects, different configurations of 16 plies laminate were investigated: Cross-ply (CP), $[90/0]_8$; Blocked-ply (BP), $[90_4/0_4/90_4/0_4]$; and Semi-blocked (SB), $[90_2/0_2/90_2/0_2]_2$. The baseline cross section area under compression was 15 x 15mm. Additionally in-plane scaled up specimens with a compression area of 30 x 30 mm, while keeping the ply thicknesses constant, were tested. Plies were cut from broadgoods material using a B&W Genesis 2100 ply cutter and lay-up was undertaken in clean room conditions following standard lay-up procedures. During lay-up a room temperature 10 minute debulk cycle was employed every four plies. Special care was taken to avoid closing the gaps between the alternating plies at the specimen sides in CP samples during debulking by inserting paper interleaves of approximately the same thickness as the plies and then removing them prior to testing. Thicknesses for the laid-up specimens were ~2.2 mm for IM7/8552, and ~3.2 mm for IMA/M21 prior to testing.

The theory of shear flow (16) suggests that for a Newtonian incompressible fluid under no-slip conditions the apparent viscosity of the squeezing material η_a (taken as the ratio between applied pressure and through-thickness strain rates) is proportional to the initial width-to-thickness ratio $(w_0/h_0)^2$. It is important to explore whether this feature is intrinsic to toughened prepregs, exhibiting elements of both shear and percolation flow and where the inter-ply conditions do not necessarily provide the no-slip interface conditions.

1.2 Test program

The baseline experimental testing was undertaken using a Metravib 2000 Dynamic Mechanical Analyser (DMA) with an iso-thermal, load-controlled compaction programme. The DMA has relatively low limits on maximum applied load and hence, this imposes constraints on the sample dimensions that can be tested at sufficiently high pressure. The effective pressurised area of the baseline samples was 15mm x 15mm, which at maximum applied load corresponds to a nominal pressure of 0.26MPa. This maximum exceeds the pressure experienced by prepregs in AFP and debulking processes but is lower than the pressure in autoclave conditions.

The range of pressures used in this investigation thus covers the pressures where changes in thickness are most important. The experimental investigation was not designed to replicate specific processing conditions, such as AFP, but to explore the compaction response of the material across a wide range of processing parameters: pressure, pressure rates, and temperatures. These parameters are characteristic for several manufacturing processes rather than AFP alone. The cylindrical boundary condition and compliance from an AFP roller, for example, are not replicated, but the rates at the ramp stage of loading are representative of the nip point of a roller. It can be expected that the state of the material tested in the ramp-dwell programme at 30°C will thus be close to the state of the material in an AFP layup, whilst the microstructure of the ramp-dwell case at temperatures between 50-90°C will be more similar to that of a prepreg stack after a hot-debulk cycle. Most of the current state-of-the-art models concentrate on attempting to replicate boundary conditions of a single ply subjected to a particular manufacturing technique (e.g. autoclave moulding). However these models will only be valid for a given manufacturing process. The set of data presented in the present publication has been used to define a generic model for toughened prepeg (see ref [10]) that can then be used to simulate any manufacturing technique of interest by applying the appropriate boundary conditions to the model. The maximum pressure rate that could be achieved by the DMA was 0.1 MPa/s. The in-plane scaled-up specimens were tested using an Instron 8801 universal testing machine with temperature controlled hot plates transferring the load and temperature to the samples, in a similar way to (17). Specimens were loaded in two regimes: a slow monotonic loading, and a ramp-dwell regime where the fast application of load is followed by long creep intervals. In both cases the baseline specimens were loaded to 60 N in 1200 seconds. For the slow monotonic case this equates to an average rate of $2.2x10^{-4}$ MPa/s. The ramp-dwell program included five 240 second steps with an incremental load of 10 N, starting at 20N. The loading rate at each step was approximately 0.1 MPa/s, comparable to the load rates seen in AFP deposition (see below for further details). The scaled-up specimens were loaded to 240 N in 1200 seconds to achieve the same effective pressure. Each sample was tested at a constant temperature throughout the loading. For the baseline specimens, this included testing at 30°C, 40°C, 50°C, 60°C, 70°C, 80°C and 90°C. The scaled-up specimens were tested at 30°C, 60°C, and 90°C. The summary of all the tests, samples and their nomenclature is given in table 2. Specimens were tested at each temperature for each material system for both monotonic and ramp-dwell cases. For the baseline specimens one test was carried out for each material system at each of the seven temperatures for the slow monotonic regime, with multiple tests at each temperature for the ramp-dwell regime. For the scaled-up cases, likewise, a single test was carried out for each material system at each of the three temperatures in the slow monotonic regime, and three tests at each temperature for the ramp-dwell programme. A thin release film was inserted between the

DMA loading plates and the samples. This film minimises friction and leads to close to the zero friction conditions at the specimen-loading interface.

A separate study was conducted to investigate whether the variability in prepreg weight has a strong influence on compaction behaviour. The cut plies were weighed before layup, with their backing sheets still attached and the weights noted. Then, lighter (below average weight) and heavier (above average weight) BP configurations of IM7/8552 were produced and tested with ramp-dwell loading.

These tests were not aimed at achieving the full fibre bed response. For the range of temperatures and short processing times, which are consistent with debulking and deposition processes, the full fibre bed response for toughened prepregs is not reached. Typically hot-debulk times are in the order of 20 minutes every 4 plies at approximately 70°C (18). At higher temperatures, above 80-90°C, the test duration was sufficient to reach a temperature independent material response, which indicates that the limit was approached.

Correction for machine compliance was made when processing the experimental results. Dummy tests were conducted with no sample, the displacement of the machine as function of the applied load was recorded and then removed from the force-displacement curve of each sample. An additional correction was needed to take into account of the uncertainty in the initial thickness. Assuming that elastic deformations are very small compared to irreversible ones, the displacement-force curves were shifted to match each sample thickness as measured immediately after the test. It should be noted that the elastic response in the through-thickness direction is not a dominant mechanism for the overall displacement and does not affect other compaction mechanisms. The study is focused on permanent irreversible deformations in the system. Table 2 shows the test matrix along with the number of tests carried out for each configuration.

Table 2. Test matrix for the experimental compaction programme.

	T(°C)	Baseline Testing					Scale-up Testing			
		CP	BP	SB	CPs	BPs	CP	BP	CPs	BPs
IM7/8552	30	4	6	1	1	1	3	3	1	1
	40	4	6	1	1	1				
	50	4	6	1	1	1				
	60	4	6	1	1	1	3	3	1	1
	70	4	6	1	1	1				
	80	4	6	1	1	1				
	90	4	6	1	1	1	3	3	1	1
IMA/M21	30	3	2	N/a	1	1	3	3	1	1
	40	3	2	N/a	1	1				
	50	3	2	N/a	1	1				
	60	3	2	N/a	1	1	3	3	1	1
	70	3	2	N/a	1	1				
	80	3	2	N/a	1	1				
	90	3	2	N/a	1	1	3	3	1	1

BP, SB, CP, BPs, and CPs denote baseline cases. A small lower case ‘s’ denotes the test has been performed under slow monotonic loading e.g. BP**s** denotes a blocked ply layup tested under slow monotonic loading. Cases without the lower case ‘**s**’ indicate ramp-dwell conditions. Scale-up specimens are denoted as BP_Scale_Up, and CP_Scale_Up. There was a greater emphasis on ramp-dwell loading since one of the key motivations for this work was model calibration and the need for understanding the material behaviour under creep conditions. Thus time dependent deformation at given loads was more important, however in-situ real-time measurements of pressure or deformation were not possible.

After testing, the specimens were cured with no applied pressure using an isothermal temperature of 100°C for 12 hours. This preserves and ‘freezes’ the internal architecture without further thickness change, as is needed for cutting and polishing of the specimen. Negligible flow of the material occurs during this process, due to the gravity only loading on what are already well compacted samples. Cutting and polishing of uncured prepreg stacks was not possible.

The widths of the ply blocks in BP and SB specimens were measured from X-ray computed tomography (CT) scans and averaged over all the specimens tested at a given temperature. For CP specimens the widths were obtained by measurements of the upper and lower surface plies using digital Vernier callipers. The specimens were then cut using a diamond coated water cooled saw and mounted in Prime20LV resin and polished for observation with light microscopy.

2. Test Results

2.1 Baseline Compaction Testing

In general, the compaction response of the prepregs follows characteristic trends for all the sample configurations and both the materials, see figure 2. Each successive loading step generated smaller and smaller displacement increments, both for the ramping and dwell stages. The final compaction displacement, at the end of the final load step, steadily increased with temperature for both loading regimes, up to about 70°C. Beyond this temperature, the thickness start to plateau and little or no further thickness reduction was seen, as shown in figure 3a (NB: CP IM7/8552 shows a slightly different trend but the displacements are much smaller than in any other configuration). This plateau thickness will be referred to here as the ‘compaction limit’. To describe the final configurations of all specimens, not just those that have reached a compaction limit, the term ‘degree of compaction’ is defined. This describes the final state of the specimen in which the extent of squeezing or bleeding may differ. It is expected that there always be some combination of the two mechanisms.

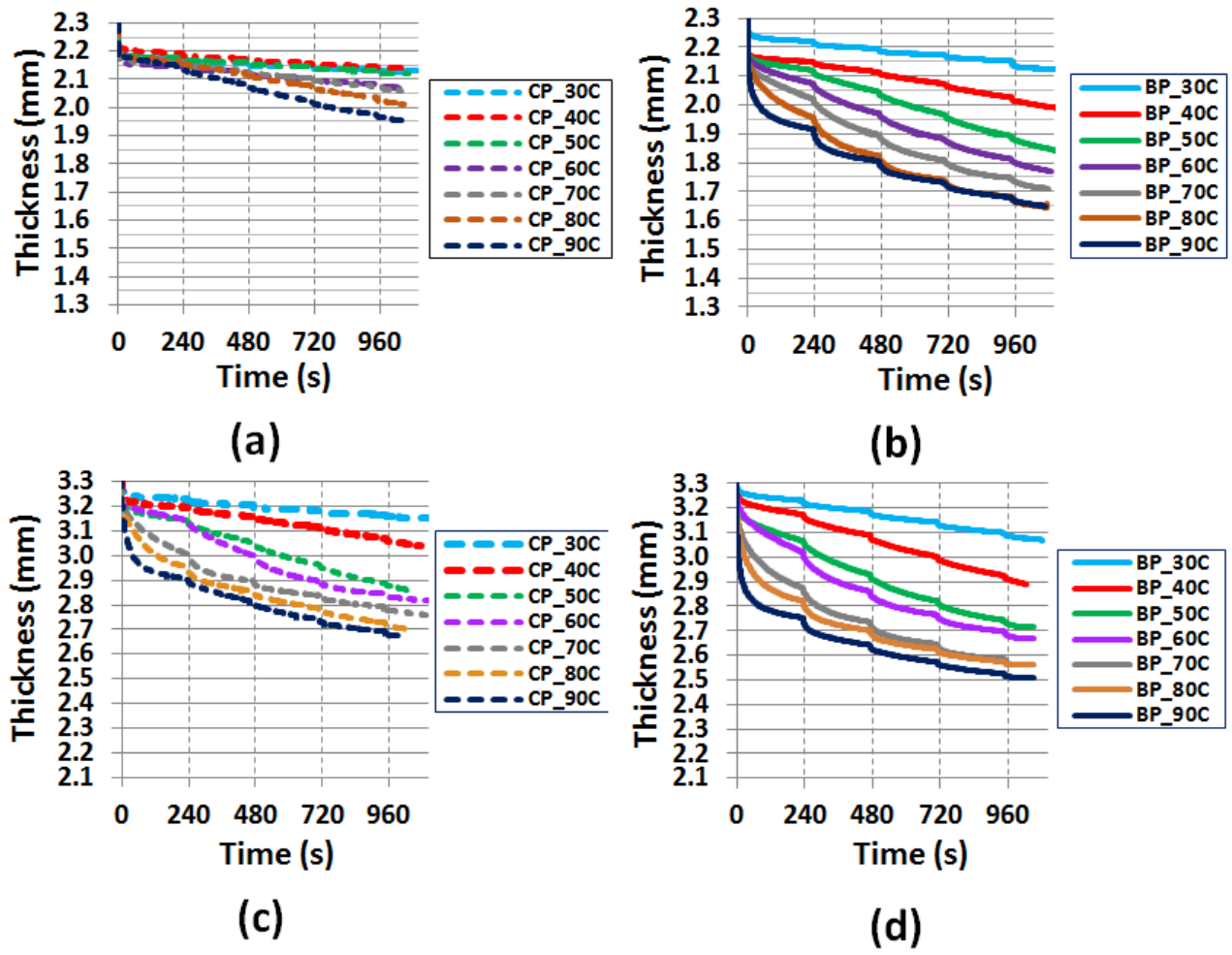

Figure 2. Thickness evolution using the baseline ramp-dwell program: (a) CP IM7/8552 (b) BP IM7/8552, (c) CP IMA/M21 and (d) BP IMA/M21.

The degree of compaction and compaction limit both show scale sensitivity and appear to be dependent on sample configuration (different for CP, SB and BP), sample size, and material system. However, the observed deformation pattern of BP samples suggested that the compaction limit is relatively invariant to initial resin viscosity at high temperatures. However the degree of compaction after the full duration of the tests is dependent on temperature across the full range and hence also resin viscosity up to a certain threshold value of temperature. There is a pronounced drop in viscosity between 70 and 90°C for BP specimens where the curves converge, which is in agreement with rheological data for the 8552 resin in (15), however for CP specimens of the IM7/8552 material, this is not strongly reflected in the curves due to the greater width to thickness ratio of the plies in the layup.

Comparing the behaviour of the two prepreg systems they were found to be quite different – Figure 3. As the nominal thickness of IMA/M21 plies is greater by a factor of ~1.5, in order for direct comparison to be made between both material systems, the final thicknesses are normalised with respect to the average of the

specimens' initial thicknesses for each configuration. The relative evolution of thickness and width in IMA/M21 is smaller compared to IM7/8552 samples. It is suggested that the main reason for this is the morphology of the toughening particles and fibre bed stiffness. However the interaction between viscosity and temperature will not change for M21/IMA as a result of the toughening particles since their size remains unaffected by the range of temperatures used in this test program. They form clear interfaces between the plies and, hence, a single ply within a block of similar orientations tends to behave more like an isolated ply rather than the whole block acting as one ply with higher thickness to width ratio. However, it was noted that for a very large number of blocked plies the merging of plies and large transfer flow may still occur.

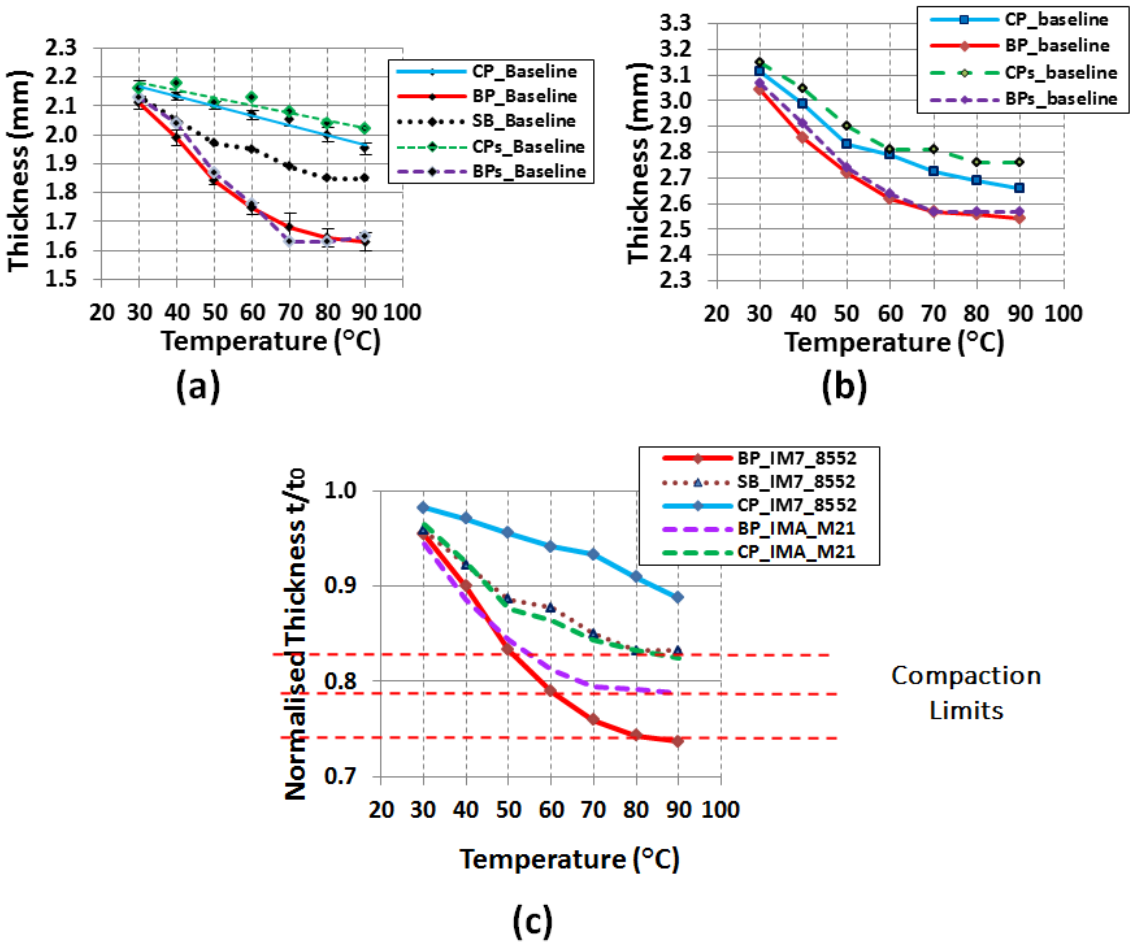

Figure 3. Absolute thicknesses for (a) Baseline IM7/8552 ramp vs monotonic, (b) Baseline IMA/M21 ramp vs monotonic and (c) Normalised baseline ramp-dwell comparison of both material systems.

2.2 Transverse widening with through-thickness compaction

As well as the changes in thickness, it is important to look at the tendency of prepregs to spread laterally to interpret the compaction response, as this shows the balance between the squeezing and bleeding mechanisms. Transverse widening and the compaction limit clearly correlate. Figures 4a and 4b show relative expansion of specimen ply widths for IM7/8552 and IMA/M21 for the ramp-dwell loading cases respectively.

The widths of BP and SB specimens are obtained by X-ray CT since the ply block widths are easily measured during post-processing of the scans. Since individual plies in CP specimens are much thinner, measurements via CT was more difficult to achieve. Instead the surface plies of CP specimens were measured at several points along the width using digital Vernier callipers. The CP samples showed almost no transverse expansion. By contrast BP and SB samples exhibited a significant squeezing flow. The squeezing deformations steadily grow in BP and SB specimens as test temperature increases up to 60-70°C. Samples tested at higher temperatures show no further width increase. Similar to the compaction limit, in figures 4a and 4b the widening limit depends on the configuration of the sample and not on resin viscosity and temperature beyond a certain threshold (~70°C). This indicates that the likely reason for the compaction/widening limits is the transition from squeezing to bleeding flow. The invariant behaviour of the limit states on resin viscosity at 70-90°C shows that by the end of tests there are greater areas of elevated fibre volume fraction throughout the specimens, coupled with a much lower proportion of load being transferred by the resin. The extent of widening/degree of compaction is dependent on resin viscosity and temperature below the threshold of ~70°C where compaction/widening limits are not always reached within the given test duration. The relation between the compaction/widening limits and sample configuration present an interesting phenomenon, which has not been extensively discussed in literature. Squeezing fluid theory predicts strong inhomogeneity of strain rate distribution under conditions of no-slip between tool and sample, as a consequence there will be a strong dependence of the apparent viscosity on the sample dimensions (width-to-thickness ratio). Indeed, CP samples were found to be two orders of magnitude more viscous than BP specimens (details on the extraction of the apparent viscosity from the ramp-dwell test are given in (10) on the modelling of these tests by the authors). Yet the viscosity alone, does not explain the convergence of the compaction curves to particular limit values. Shear flow theories do not foresee any compaction limit other than the case when sample thickness approaches zero and the apparent viscosity becomes infinite due to the assumption of perfectly aligned parallel fibres. This observation evidences that the transverse flow may have a certain strain limit. Barnes and Cogswell (19) observed similar compaction restraints for reinforced thermoplastics and suggested that twisting of fibres at the flow front may cause the spreading locking. However, a compaction limit state is typical for bleeding low viscosity systems as shown by Gutowski and Dilan [5].

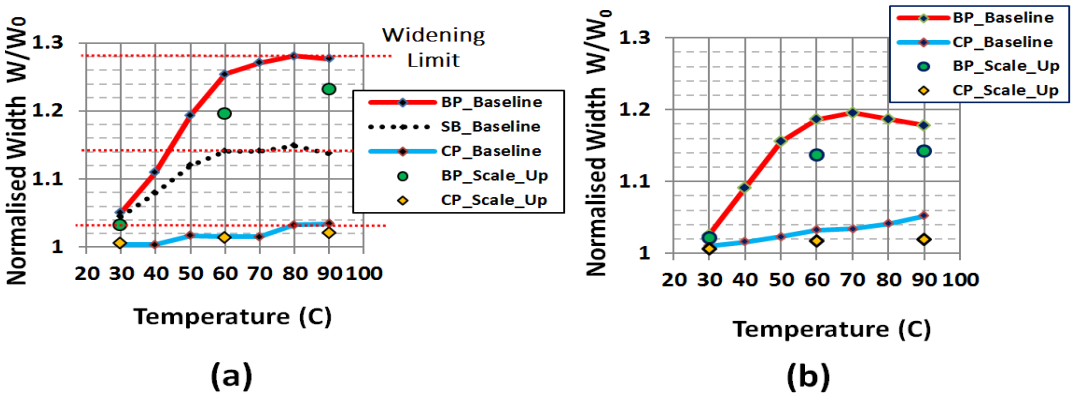

Figure 4. Relative expansion of specimen ply widths for (a) IM7/8552 and (b) IMA/M21.

Figure 5 shows the average extent of the transverse spreading behaviour for each ply block through the thickness for BP baseline tests for IM7/8552 and IMA/M21 at each temperature. It is shown that there is considerably greater spreading behaviour for the inner ply blocks especially at elevated temperatures, due to the partial slip condition between the plates and the specimen (enhanced by the applied pressure) and lower friction between the plies, which demonstrates the importance of the tool/layup interaction during pre-curing consolidation.

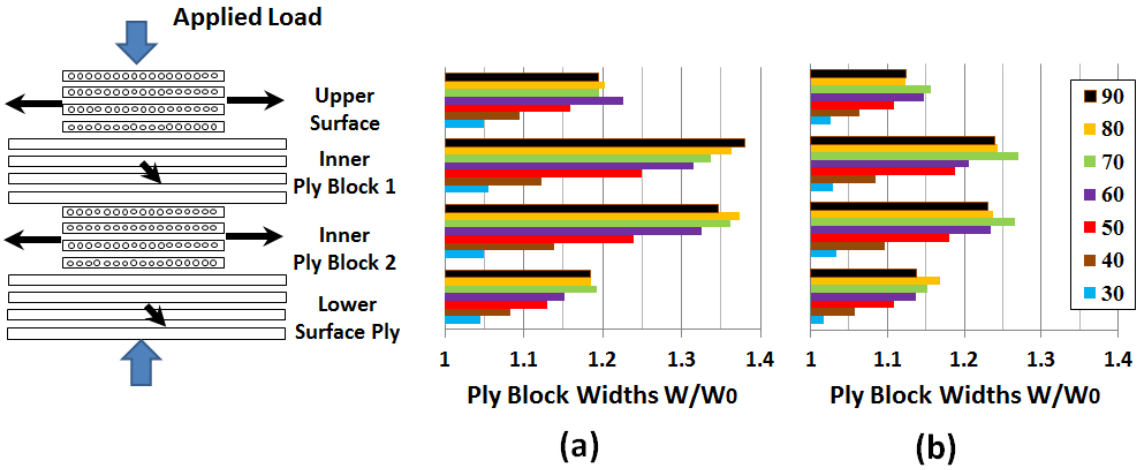

Figure 5. Relative expansion of ply widths for ramp-dwell baseline BP (a) IM7/8552 and (b) IMA/M21 specimens.

2.3 History and strain-rate effects

Comparison of slow monotonic and ramp dwell programs (with the same average load rate and maximum load level) was made to assess the effect of strain rates on spreading. Previously it was found that for a very high thickness to width aspect ratio, T700/M21 prepreg material showed pronounced differences in resultant thickness for different loading programs [8]. For the current sample configurations with a smaller number of

plies blocked together no notable difference in transverse expansion and through-thickness compaction of the specimens for slow monotonic loading versus ramp-dwell loading for IM7/8552 was found. Initially the ramp-dwell case shows a larger decrease in thickness due to greater squeezing flow and greater load rates at the beginning of each step, with monotonic loading giving a more gradual trend in the thickness evolution. Both loading regimes reach similar values of final thickness for each temperature at the end of the test. Figure 6 shows a comparison of thickness-time curves for the baseline BP specimens under monotonic loading to the ramp-dwell case for 30°C, 60°C, and 90°C.

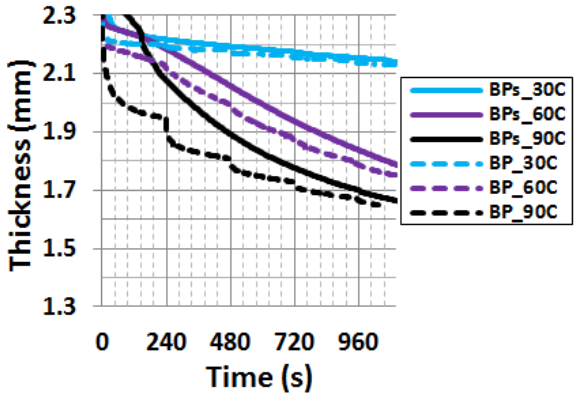

Figure 6. Variation in thickness with slow monotonic loading compared to the ramp-dwell case for baseline IM7/8552 BP Specimens.

2.4 The Effect of Variability in Plies

To investigate a possible correlation between compressibility and variation in prepreg areal weight, "light" and "heavy" versions of the IM7/8552 BP specimens were produced and tested at the various temperatures. 224 plies cut to size were weighed with their backing sheets attached and sorted by weight. Plies which had an above average weight were designated for layup of the 'heavy' specimens and those below average weight were used for the 'light' specimens. The specimens made from the 'heavy' plies had a 3.2% greater mass than the lighter specimen. The mean specimen weight for standard BP specimens from batch 4 was 1.22g with a CV of 0.78%, for light BP specimens: 1.20g (CV of 0.39%), and for heavy BP specimens: 1.24g (CV of 0.28%). Figure 7 shows the average final thicknesses for BP specimens in blue with standard deviation error bars, along with the result for the light and heavy BP specimens. The results indicate that the final thicknesses are well within the normal range of scatter for the experimental programme and hence, the observed variation in weight cannot be said to impact on measured material response.

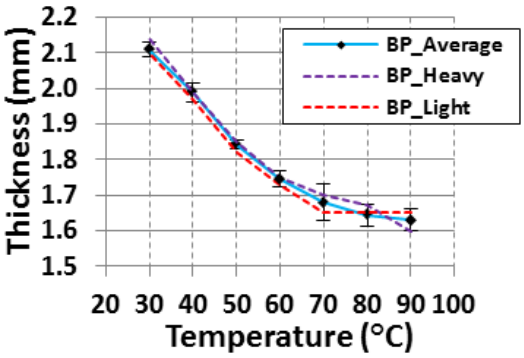

Figure 7. Thickness variation in light and heavy specimens for baseline BP specimens using IM7/8552 under ramp-dwell loading.

2.5 Scale-up Compaction Testing

The scale-up tests show a similar material response in comparison to the baseline cases. As with the baseline case, squeezing behaviour was predominantly seen in ramp-dwell tests for elevated temperatures. However there is a notable size effect in which the larger samples show reduced through-thickness displacements compared to the baseline specimens. From (16) it can be deduced that the apparent viscosity is highly dependent on the initial width to thickness ratio, thus for a given applied through-thickness strain the resulting transverse strains and hence the extent of squeezing flow will be lower for greater in-plane dimensions. Therefore giving rise to the reduced through thickness displacements seen in the scale-up tests. Final thicknesses were normalised by the initial thicknesses for baseline and scale-up tests with IM7/8552 and IMA/M21 specimens plotted in figures 8 (a) and 8(b) respectively.

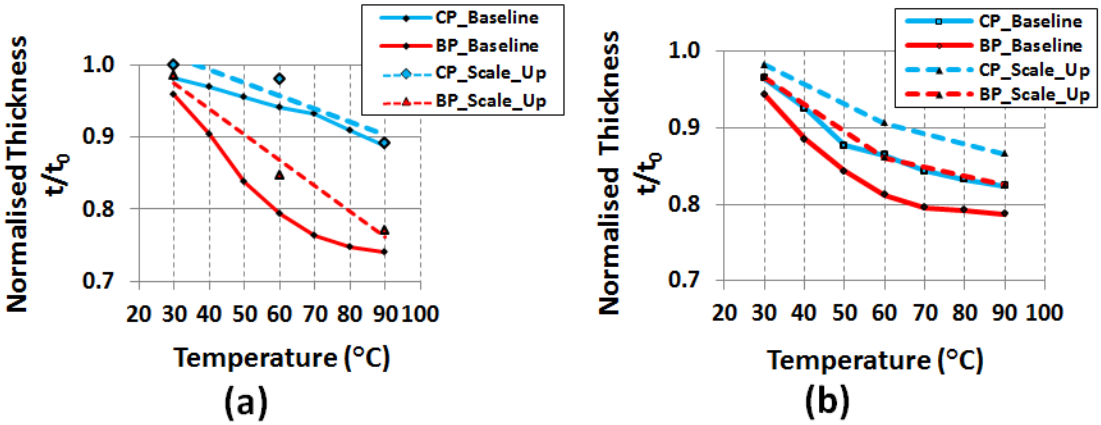

Figure 8. Normalised comparison of scale-up thickness curves for ramp-dwell loading (a) IM7/8552 and (b) IMA/M21.

2.6 Microstructure of compacted samples

The microstructures of the prepregs experience a significant transformation over the course of compaction. The examination of the cross-section of cured samples gives further insight into the deformation mechanisms. A

summary of micrographs of specimens subjected to ramp-dwell compaction is given in figure 9. Several features in these micrographs are worth emphasizing:

Extensive inter- and intra-ply voids, along with areas of low fibre density can be seen prior to compaction testing. Compaction at low temperatures (30°C) neither fully suppresses voids nor changes the characteristic dimensions of them (NB: in actual component manufacture the material is compacted under vacuum which assists in eliminating voids. The analysis given here is purely to characterise the specimen deformation).

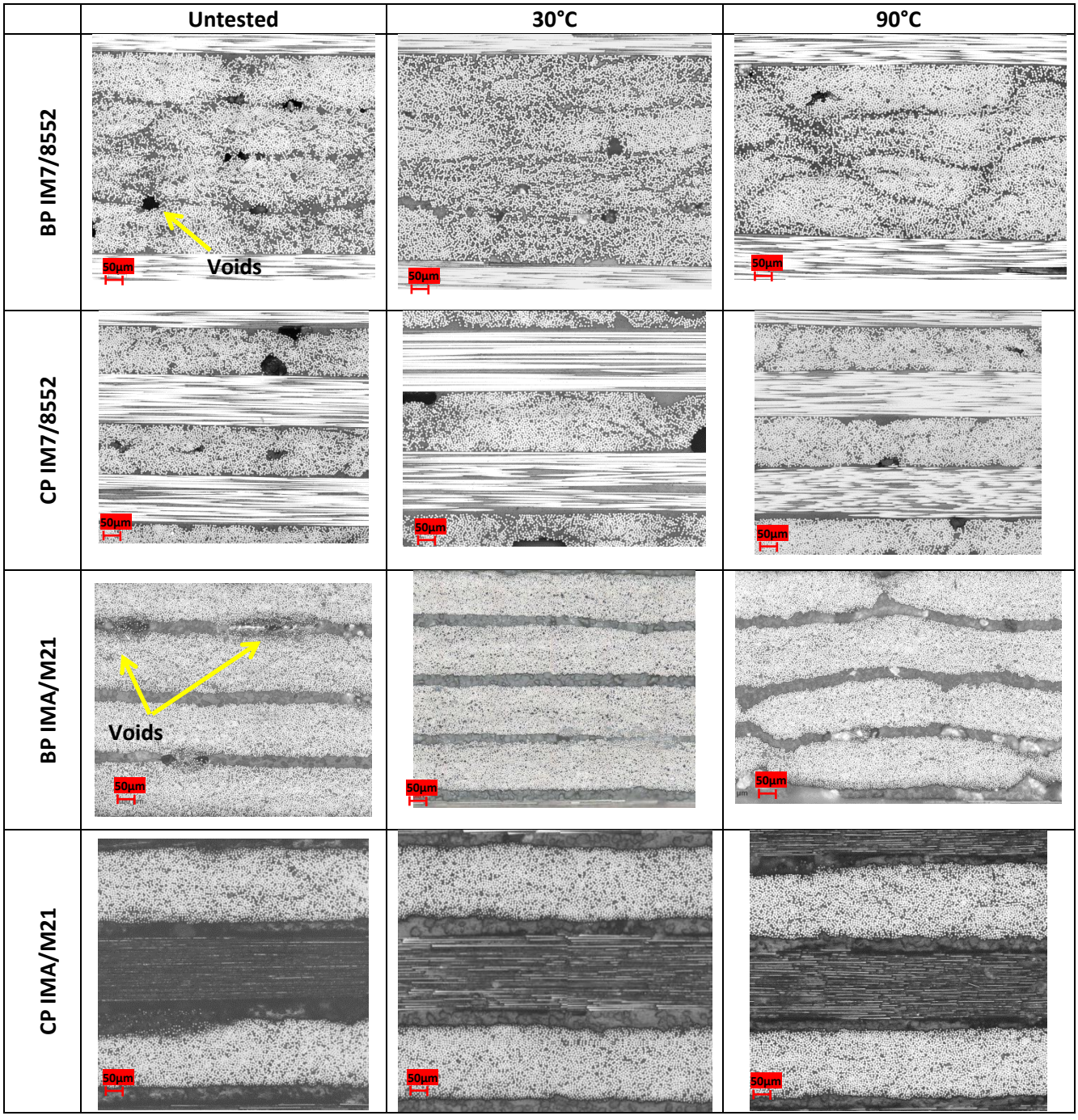

Figure 9. Summary of Micrographs.

Samples tested at high temperatures tend to show both reduced void size and reduced amount of low fibre density areas. Voids tend to increase in size towards the edge, which is in agreement with squeezing flow theory predicting higher pressure away from the edges.

A clear interface (thin resin rich layer) between plies of the same orientation prior to testing could be seen. In IM7/8552 BP specimens the inter-ply boundaries merge and become more distorted after compaction (figure 10). The interface was still detectable, but its geometry presents a complex irregular path through the thickness of nested plies (details inset on Figure 10). A degree of distortion of inter-ply boundaries was also seen in the IMA/M21 specimens, however, the degree of distortion was much less than for IM7/8552. The inter-ply layer of thermoplastic particles, which are characteristic of this material system, remained clearly visible. This can explain why BP and CP specimens for this material show greater similarity in final thicknesses after compaction than for IM7/8552. Each ply in the ply block of BP specimens behaves more like it was in isolation, whereas in IM7/8552 the plies in a given block are merged in a squeezing flow. The degree of nesting, judged by the distorted geometry of ply interfaces, is higher at elevated temperatures for both the materials.

The resin tends to flow predominantly along the fibre direction via channels in between the fibre tows and out via the interfaces between plies. The bleeding flow mechanism is observed upon approaching a compaction limit where the pressure gradient begins to cause resin flow independently of the fibre bed. Traces of transverse bleeding were noticed in CP samples at 90°C, evidenced by displacement of fibres at the edges, in IM7/8552 (figure 11). Evidence of bleeding flow is also observed in IMA/M21 CP samples at 90°C in which toughening particles are carried from the interleaves (figure 12).

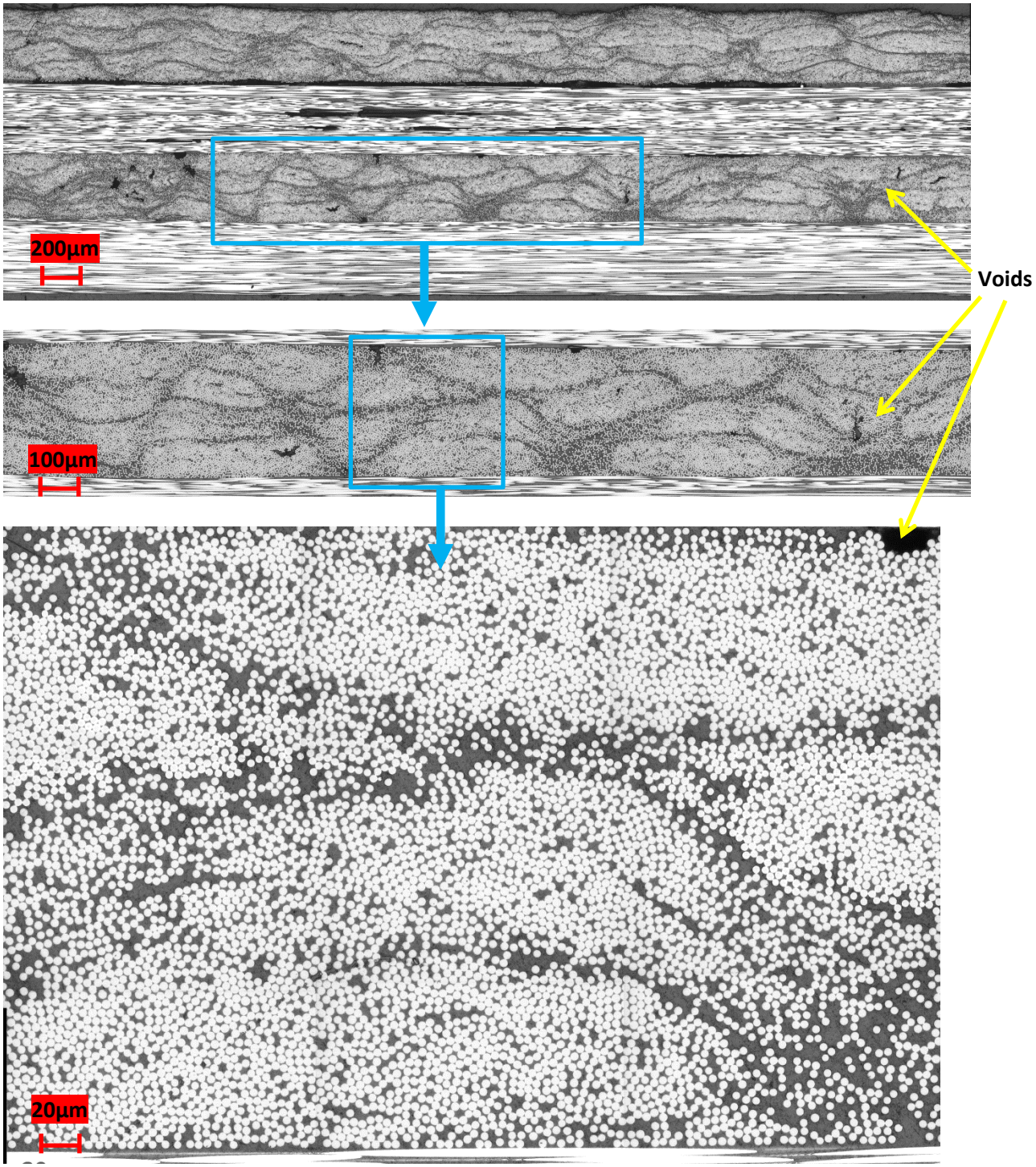

Figure 10. BP at 90°C for IM7/8552.

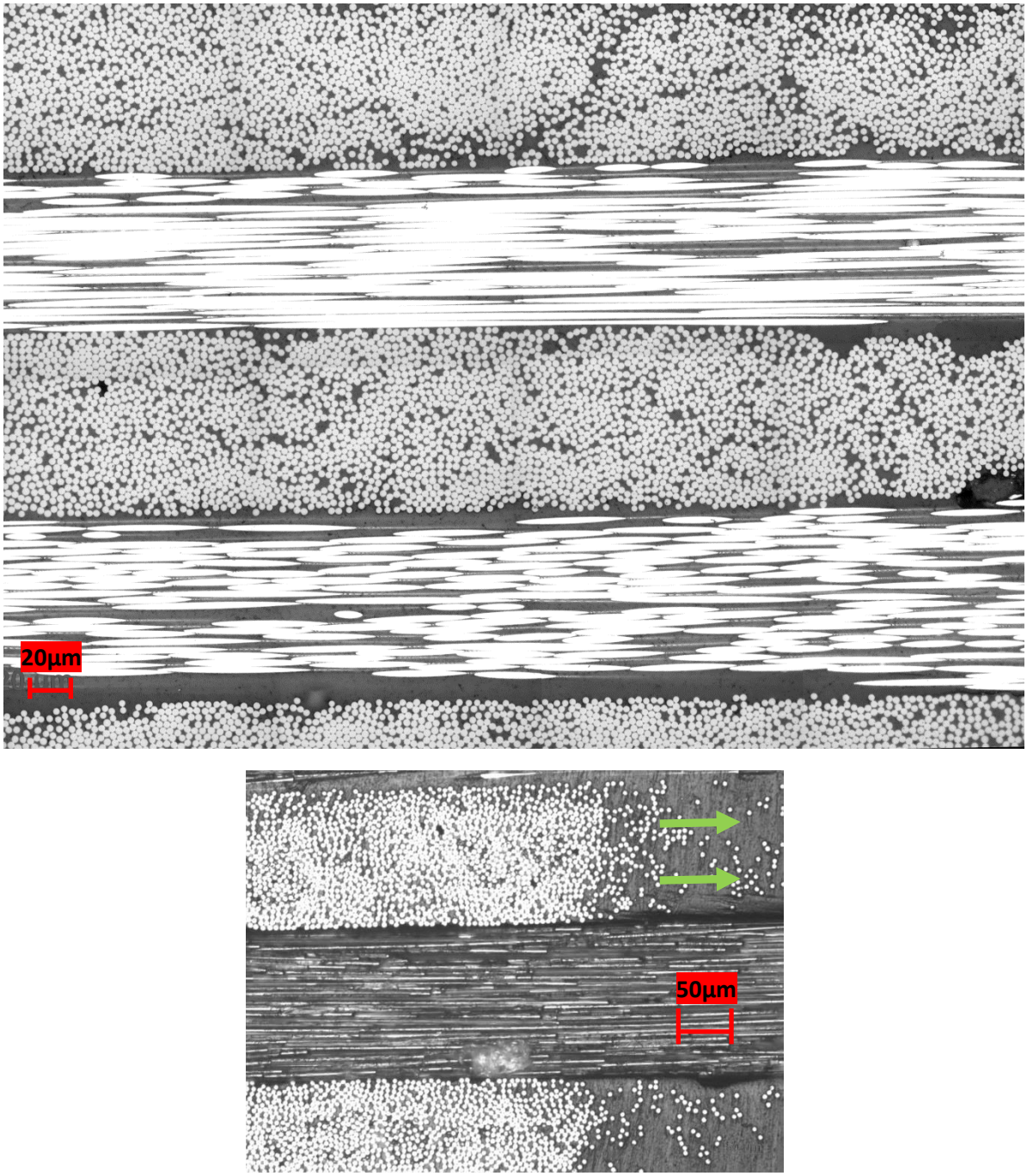

Figure 11. CP 90°C for IM7/8552.

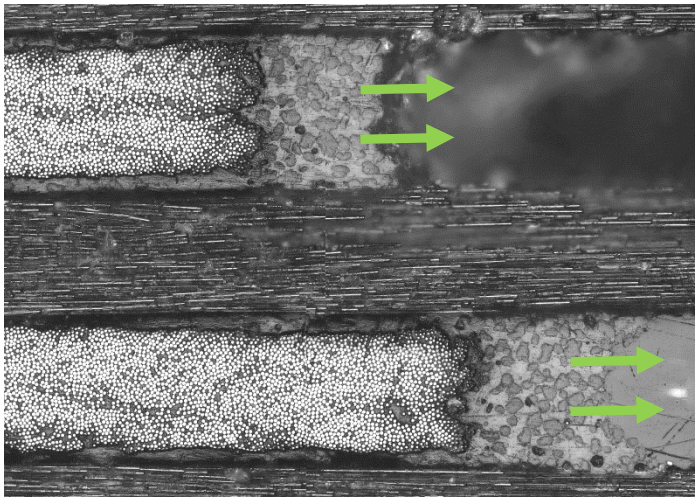

Figure 12. CP 90°C for IM7/8552.

3. Discussion and Conclusion

A comprehensive range of compaction experiments and characterisation has been presented in order to further understand the nature of toughened prepregs during the compaction phase of the manufacturing process. It is shown how the apparent viscosity of the specimens made from two different prepreg materials with notably different morphologies, is highly dependent on the initial geometry of the specimens and the layup. A scaling effect is observed upon increasing the in-plane specimen dimensions. Thus there is a notable size effect in both the in-plane and through-thickness directions for both material systems in which the compaction is dependent on the thickness to width ratio. The incompressibility assumption implies that the applied through thickness strains are equivalent to the transverse strains for a ply or ply block. (Whilst dry fibre regions and voids may be filled by resin at higher temperatures reducing the overall specimen volume without mass loss, this effect is likely to be negligible in terms of the incompressibility assumption since the void content was found to be less than 2% from X-ray CT scans). Thus if the ply thickness increases (for instance in going from CP to BP) the width to thickness ratio is lower, hence the transverse strains are greater, explaining the greater spreading behaviour for BP for a given temperature. If the in-plane dimensions increase for a given configuration then the transverse strains are comparably lower for the same applied through thickness strain.

An evaluation of the microstructure gives very clear evidence of the squeezing flow mechanism through inter-ply distortion between ply-blocks. It also shows how the morphology of the prepreg can have a notable effect on the compaction behaviour. In IMA/M21 the thermoplastic particles have an inhibiting effect on this flow mechanism however the compaction response of the material still shows clear features of bleeding flow.

The results show that both of the toughened material systems investigated here exhibit bleeding and squeezing flow mechanisms. As well as the micrographic evidence, results reveal features expected for both the flow

types. The observations show that for the sample sizes, test durations and strain rates selected for this test programme, the compaction and widening limits are independent of temperature and thus viscosity above a certain temperature threshold, which was found to be ~70°C, where the compaction curves converge to give a compaction limit. Below this threshold, for temperatures between 30-60°C, the degree of compaction is dependent on temperature and viscosity. The coupling of squeezing and bleeding flow in application to prepregs systems has rarely been discussed in literature and available models cannot be readily adopted. Furthermore, prior to bleeding/percolation modern prepreg materials show important features, which are not covered by standard squeezing flow models. Thus, the experiments reveal a requirement for a new material description, which is presented in a separate publication by the authors and describes a 3D hyper-viscoelastic material model (10) which can:

- Describe samples of arbitrary thicknesses by the same governing equation(s)
- Explicitly include the geometrical size effects in the formulation
- Capture the thickness change, which starts to approach the compaction limit at elevated temperatures.
- Take into account the strain-rate dependency
- Employ material constants which can be derived from the compaction tests
- Be at the ply scale, and be deployable in a ply-by-ply finite element analysis.

Model parameters were identified from this experimental programme and validated against compaction experiments using the same range of load rates, temperatures, and laminate configurations as in this paper.

Acknowledgements

This work has been funded by the EPSRC Centre for Innovative Manufacturing in Composites project "Defect Generation Mechanisms in Thick and Variable Thickness Composite Parts - Understanding, Predicting and Mitigation" (EP/I033513/1). Supporting data may be requested from Prof. S. R. Hallett. Access to supporting data may be granted, subject to consent being requested and granted from the original project participants.

References

1. Lukaszewicz DH-JA. Considerations for automated layup of carbon-fibre thermoset preimpregnates, : PhD Thesis, University of Bristol; 2011.

2. Ivanov D, Li Y, Ward C, Potter K. Transitional behaviour of prepregs in Automated fibre deposition processes. Proceedings of the 19th International Conference on Composite Materials, Montreal 2013.

3. Hélénon F, Ivanov D, Potter K. Modelling slit tape deposition during automated fibre placement. Proceedings of the 19th International Conference on Composite Materials; Montreal 2013.

4. Hubert P, Poursartip A. Aspects of the Compaction of Composite Angle Laminates: An Experimental Investigation. Journal of Composite Materials. 2001;35(1):2-26.

5. Gutowski TG, Dillon G. The Elastic Deformation of Lubricated Carbon Fiber Bundles: Comparison of Theory and Experiments. Journal of Composite Materials. 1992;26(16):2330-47.

6. Hubert P, Poursartip A. A method for the direct measurement of the fibre bed compaction curve of composite prepregs. Composites Part A: Applied Science and Manufacturing. 2001;32(2):179-87.

7. Buntain MJ, Bickerton S. Modeling forces generated within rigid liquid composite molding tools. Part A: Experimental study. Composites Part A: Applied Science and Manufacturing. 2007;38(7):1729-41.

8. Kelly PA. A viscoelastic model for the compaction of fibrous materials. The Journal of The Textile Institute. 2011;102(8):689-99.

9. Lukaszewicz DH-JA, Potter K. Through-thickness compression response of uncured prepreg during manufacture by automated layup. Proceedings of the Institution of Mechanical Engineers, Part B: Journal of Engineering Manufacture. 2012;226(2):193-202.

10. Belnoue JP-H, Nixon-Pearson OJ, Hallett SR, Ivanov DS. A Novel Hyper-Viscoelastic Model for Consolidation of Toughened Prepregs under Processing Conditions. Mechanics of Materials. 2016; 97: 118-134.

11. Lukaszewicz DHJA, Potter KD. The internal structure and conformation of prepreg with respect to reliable automated processing. Composites Part A: Applied Science and Manufacturing. 2011;42(3):283-92.

12. Hubert P, Johnston A, Poursartip A, Nelson K. Cure Kinetics and Viscosity Models for Hexcel 8552 Epoxy Resin. In: International SAMPE Symposium and Exhibition (Proceedings), (2001), Vol 46, pp 2341-2354.

13. Hexcel HexPly 8552, Epoxy Matrix Product Datasheet. pdf download from: www.hexcelcomposites.com/Markets/Products/Prepreg/PrepregDownld.html.

14. Hexcel HexPly M21, Epoxy Matrix Product Datasheet. pdf download from: http://www.hexcel.com/Resources/DataSheets/Prepreg-Data-Sheets/M21_global.pdf.

15. Van Ee D, Poursartip A. HexPly 8552, Material Properties Database for use with COMPRO CCA and Raven, National Center for Advanced Materials Performance. 2009.

16. Rogers TG. Squeezing flow of fibre-reinforced viscous fluids. J Eng Math. 1989;23(1):81-9.

17. Rouhi MS, Wysocki M, Larsson R. Experimental assessment of dual-scale resin flow-deformation in composites processing. Composites Part A: Applied Science and Manufacturing. 2015;76:215-23.

18. Campbell FC. Chapter 5 - Ply collation: A major cost driver. In: Campbell FC, editor. Manufacturing Processes for Advanced Composites. Amsterdam: Elsevier Science; 2003. p. 131-73.

19. Barnes JA, Cogswell FN. Transverse flow processes in continuous fibre-reinforced thermoplastic composites. Composites. 1989;20(1):38-42.